10TH INTERNATIONAL SYMPOSIUM ON PARTICLE IMAGE VELOCIMETRY - PIV13
Delft, The Netherlands, July 1-3, 2013

Systematic timing errors in laser-based transit-time velocimetry

Philippe M. Bardet[1], **Matthieu A. André**[1] **and Douglas R. Neal**[2]

[1]Department of Mechanical and Aerospace Engineering, The George Washington University, Washington, DC, USA
bardet@gwu.edu

[2]LaVision Inc, Ypsilanti, MI, USA
dneal@lavisioninc.com

ABSTRACT

Laser diagnostics for measuring velocity or acceleration are based either on transit-time or Doppler effect. Transit-time techniques rely on the displacement of tracers during a given amount of time. Tracers can be either particles (Particle Image Velocimetry, Particle Tracking Velocimetry) or molecules (Molecular Tagging Velocimetry). In these diagnostics, the velocity or acceleration is controlled by the timing of lasers that are used in dual, triple, or quadruple pulse mode. Of all the sources of uncertainties associated with these techniques, timing has been considered negligible except for occasional misfires or very high-speed flows ($\geq$ 10 km/s). However, in Q-switched lasers, such as Nd:YAG or Nd:YLF, a systematic bias was measured between the triggered pulse separation (Δt) and actual pulse separation values. Several different lasers from various manufacturers were characterized and it was found that the timing uncertainty has a complex relation to the laser power, frequency, and in some cases the triggered Δt. When such lasers are used in a dual cavity configuration, errors vary up to 0.5 μs and up to 1 μs for single cavity lasers with dual pulse capabilities. Such large discrepancy can lead to very significant systematic errors in measurements. The various reasons for these discrepancies are discussed and several different approaches are proposed to measure and correct this source of uncertainty.

1. Introduction

Particle image velocimetry (PIV) is an established technique capable of reliably measuring fluid velocities fluid flows. Recently the usage of PIV has evolved beyond the expert user in the fluid dynamics research community and now PIV systems are routinely being used by fields as diverse as oceanography, biology, and zoology along with both food and medical science. This widespread acceptance has helped to create an interest in being able to assess the experimental uncertainty on an instantaneous vector map, essentially the desire to put ”error bars” on each PIV vector. These uncertainty efforts are primarily concentrated on quantifying the random and bias errors associated with accurately determining the distance the particles traveled, Δs, over a known amount of time, Δt (e.g. [1, 2, 3, 4, 5]). However, given the precision of timing electronics from reliable commercial sources, the uncertainty of the denominator, Δt, has been assumed to be a negligible factor. This assumption of negligible timing uncertainty does not account for the complex physics associated with the actual lasing process and the subsequent release of the laser energy. PIV lasers are in fact complex dynamic systems that have inherent latencies associated with a specific laser or laser cavity. This fact is further complicated by the different types of lasers that are commercially available. Some of these lasers offer clever Q-switching schemes to allow for a single cavity laser to be used in a frame-straddling or dual pulse mode. This work shows a thorough investigation of the timing issues of a wide range of commercially available PIV lasers. The bias errors introduced by the Q-switches of various lasers are both characterized and quantified. Recommendations to mitigate these bias errors are presented.

In transit-time measurements, the displacement of tracers (either particles or molecules) is followed in time and the velocity extrapolated. Such measurements rely on precise timing of the illumination source or the imaging sensor. In particle image velocimetry (PIV), and likewise, in particle tracking velocimetry (PTV) and molecular tagging velocimetry (MTV), pulsed lasers are commonly used and the timing uncertainties have been usually neglected except for occasional misfires and very high-speed flows [6]. We report data for several lasers where systematic timing uncertainties can vary by up to more than 1 μs .

In PIV, the Eulerian fluid velocity is related to the Lagrangian velocity [6]:

$$\mathbf{U}(\bar{\mathbf{x}}_p, t^*) = \frac{\Delta \mathbf{x}_p}{\Delta t} + \left(\bar{\mathbf{x}}_p - \mathbf{x}_p(t^*)\right) \cdot \nabla \mathbf{u}|_{\mathbf{x_p}} - \left(\dot{\mathbf{v}}_\mathbf{p}(t^*) - \mathbf{b}\right) \tau_p - \frac{1}{24} \ddot{\mathbf{v}}_\mathbf{p}(t^*) \Delta t^2 + O(\Delta t^4) \tag{1}$$

where $\bar{\mathbf{x}}_p = (\mathbf{x}_p(t) - \mathbf{x}_p(t+\Delta t))/2$ is the mean particle location and $t^* = t + \Delta t/2$ the mid-time between the two pulses, Δt the pulses separation. In eq. (1) right hand side (RHS), the first term is the Lagrangian velocity and the last three terms are correction introduced by the flow field.

Uncertainties in the Lagrangian velocity, or first term in eq. (1) RHS, depend on image center error, magnification, and timing:

$$\left(\frac{\delta(\Delta x_p/\Delta t)}{(\Delta x_p/\Delta t)}\right)^2 = \left(\frac{\delta x_p}{x_p}\right)^2 + \left(\frac{\delta M_\circ}{M_\circ}\right)^2 + \left(\frac{\delta \Delta t}{\Delta t}\right)^2 \tag{2}$$

This timing uncertainty (eq. (2) last term on RHS) dominates the overall timing uncertainty in the Eulerian velocity, eq. (1). Hence, systematic timing errors have first order dependence on the calculated velocity in PIV. Likewise, in PTV and MTV, timing errors are first order terms.

Vorticity is a variable of prime interest when studying fluid dynamics. Vorticity being calculated by differentiating the velocity, the error in velocity propagates to the vorticity. The general expression for the spatial derivative at a point j based on a central scheme of order n is [7]:

$$\left.\frac{\partial u}{\partial x}\right|_j = \frac{1}{a\Delta x}\sum_{i=1}^{n/2} a_i(u_{j+1}-u_{j-1}) + \sum_{i=n+1}^{\infty} \alpha_i \frac{\Delta x^{i-1}}{i!}\left.\frac{\partial^i u}{\partial x^i}\right|_j + \varepsilon\frac{\sigma_u}{\Delta x} \tag{3}$$

The term on the left side is the exact derivative. The first term on the right is the approximate value calculated by a given scheme. The second term on the right is the truncation error. The truncation error decreases as the order of the scheme increases. The last term is the error coming from the velocity error σ_u. An amplification coefficient ε arises which depends on the order of the scheme. It takes the value of 0.71, 0.95, 1.08 or 1.17 for a scheme of order 2, 4, 6, or 8, respectively. Therefore, the error on the velocity due to the timing which is of the first order, is also introducing a first order error on the vorticity.

Nd:YLF and Nd:YAG lasers from several manufacturers have been tested. It is confirmed that jitter is very low, but the delay between the trigger and laser pulses varies with laser power and operating frequency. Procedures to correct for these timing errors are presented as well as potential explanation regarding the error sources.

2. Dynamics of Q-Switched Lasers

For transit-time velocimetry, the most commonly employed lasers are pulsed Q-switched solid-state lasers, such as neodymium-doped yttrium aluminum garnet (Nd^{3+}:YAG or simply Nd:YAG) or neodymium-doped yttrium lithium fluoride (Nd^{3+}:YLF or Nd:YLF). For low speed flows, however, it is possible to use CW lasers [8], which of course are not affected by the same dynamic behavior.

Both Nd:YAG and Nd:YLF lasers are four-level lasers, Fig. 1, and following derivation of Svelto [9] only the main results on the dynamics of four-level Q-switched lasers will be presented. By modulating damping or losses in laser cavity, $\gamma(t)$, it is possible to build a large, or surplus, population inversion (atoms in high energy level) by optical pumping and then release a short and high-energy pulse when the cavity losses are low. This is referred as Q-switching. In the subsequent analysis the switching of the cavity from a high to low losses is assumed to be instantaneous; however, in practice this is not always the case, which leads to slightly different behaviors, in particular longer pulses than predicted here.

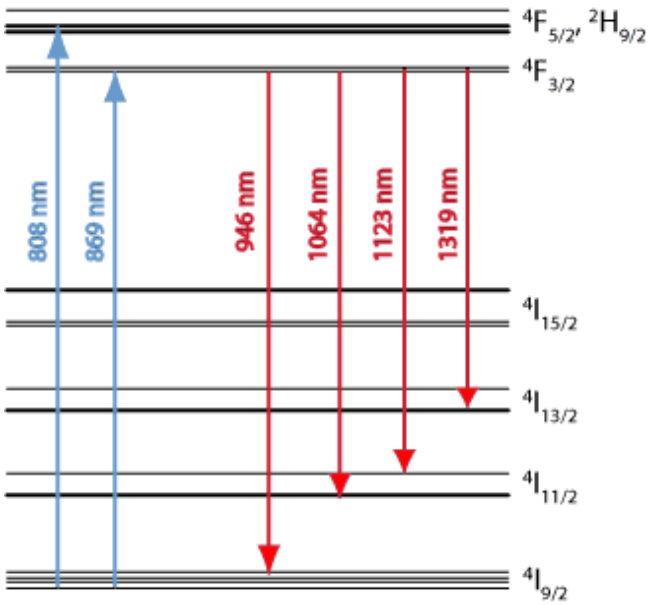

Figure 1: Energy levels in YAG lasers. Most common YAG emission is 1064 nm, [10].

Active Q-switching is typically operated in two modes depending on the pumping mode: pulsed or continuous pumps. The rise time of laser pulses is related to the surplus inversion, while the falling time depends on the photon lifetime inside the resonator, τ_c (eq. 4). This varies from a few nanoseconds to tens of nanoseconds.

2.1 Pulsed pump Q-switch

Pulsed pump lasers are typically pumped by flashlamps and operate from few Hz to few tens of Hz. Most common Q-switches are now electro-optical modulators, which consist of Pockels cells. Pockels cells are made of crystal with refractive index that is proportional to applied electrical field strength. By applying an electrical voltage to the crystal, it is possible to retard the phase of the light propagating in the crystal and hence create high-losses in the laser resonator [10].

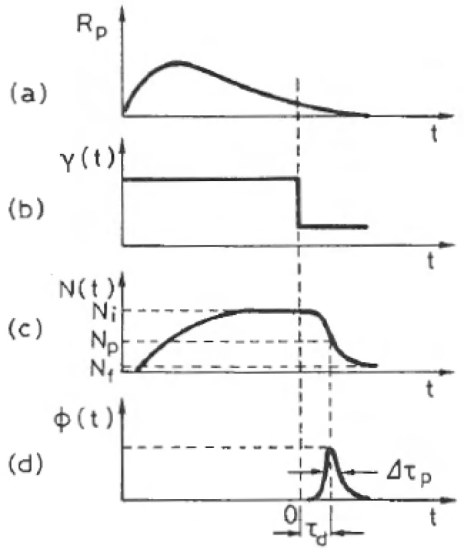

Figure 2: Behavior of pulsed pump Q-switch laser. (a) R_p is the pump rate, (b) $\gamma(t)$ the losses in the laser cavity, (c) $N(t)$ the number density of atoms in upper-state, and (d) $\phi(t)$ cavity photon number [9].

The photon decay time in the cavity, τ_c, is related to the cavity effective length, L_e, and the resonator losses, γ:

$$\tau_c = -\frac{L_e}{c\gamma} \tag{4}$$

where c is the speed of light. τ_c is typically a few to tens of nanoseconds.

The amount by which the lasing threshold is exceeded, x, is the ratio of the initial pump energy just before the pulse, N_i, to the critical or threshold pump energy for lasing, N_c. This last term corresponds to the population inversion necessary to overcome losses in the cavity, $N_c = \gamma/\sigma l$, with σ the stimulated emission cross section, and l the crystal length. For pulsed pump Q-switch, N_c also equals to inversion population at the pulse peak power, N_p:

$$x = \frac{N_i}{N_c} = \frac{N_i}{N_p} \tag{5}$$

The initial inversion population is equal to the product of the upper-state or fluorescence lifetime, τ, and the pumping rate at the time of Q-switching, $Rp(0)$, following the notations of Fig. 2:

$$N_i = R_p(0)\tau \tag{6}$$

At first order a given flashlamp has similar temporal response regardless of the level of excitation voltage. This implies that the total pump energy is proportional to $R_p(0)$. Therefore N_i is directly related to the pump energy, which in turn depends the excitation voltage.

The pulse width, $\Delta\tau_p$, is typically 1.5 to 5 the cavity decay time, τ_c:

$$\Delta\tau_p = \tau_c \frac{(N_i/N_p)\eta_E}{\left[(N_i/N_p) - \ln(N_i/N_p) - 1\right]} \tag{7}$$

with $\eta_E = (N_i - N_f)/N_i$ the energy utilization factor and N_f the inversion population at the end of the pulse, Fig. 2.

The time delay or pulse buildup time, τ_d, is set as the interval between the Q-switching time and peak of laser pulse, Fig. 2:

$$\tau_d = \frac{\tau_c}{x-1} \ln\left(\frac{\phi_p}{10}\right) \tag{8}$$

where ϕ_p is the number of photons at the peak of the pulse: ϕ_p increases with increasing excess threshold energy, x. As the pumping rate, R_p, is decreased, x will also decrease, which according to (eq. 8) will result in longer buildup time. Likewise, the pulse length will also increase with decreasing pumping rate (eq. 7). These results are summarized in Fig. 3 for a hypothetical laser.

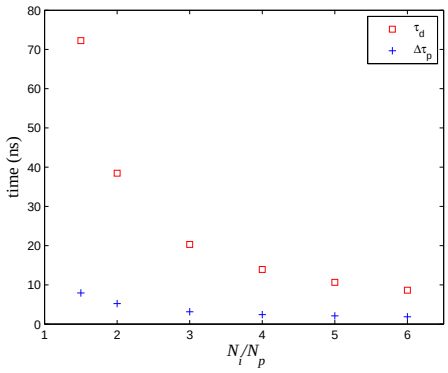

Figure 3: Behavior of laser pulse width, $\Delta\tau_p$ and buildup time for pulsed pump, τ_d, after [9].

Finally, fast switching implies that the switching time is shorter than the buildup time, this is often hard to accomplish with short cavities as it takes time to turn off a 1-5 kV electrical pulse. Typically this can be accomplished in less than a 1 ns. As a result, pulse length is usually longer than predicted with model above.

2.2 Continuous pump Q-switch

High power LEDs are employed to continuously pump laser cavity. For these lasers, long upper-state, or fluorescence, lifetime τ is particularly desirable to obtain a large population inversion with relatively low pump power and store a large amount of power. With this pumping scheme, repetition rates are in the kHz to tens of kHz range and Q-switches are acousto-optics modulators where the refractive index of the crystal is modulated by the pressure exerted by RF acoustic waves. The acoustic waves are typically imparted to the crystal with a piezoelectrical material connected to the crystal. For Nd:YLF, the fluorescence lifetime is $\tau = 485\ \mu$s for 1% Nd doping; for Nd:YAG $\tau = 230\ \mu$s for 1% Nd doping. Nd:YLF crystals longer lifetime than Nd:YAG makes them more suitable for 1-10 kHz range, and Nd:YAG crystals are employed for higher frequencies.

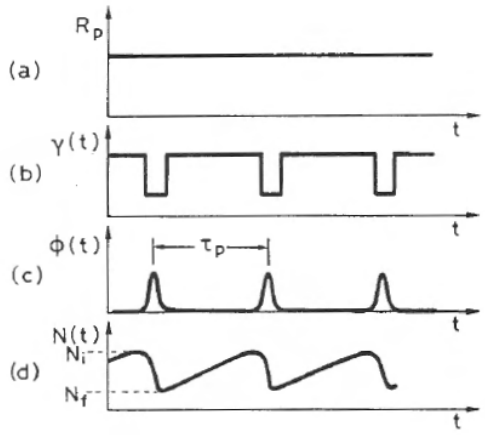

Figure 4: a) R_p is the pump rate, (b) $\gamma(t)$ the losses in the laser cavity, (c) ϕ cavity photon number , and (d) N the number density of atoms in upper-state, [9].

Due to the different pumping scheme, Fig. 4 (a), the laser behaves differently. Most notably, to rebuild the initial inversion population, N_i, the cavity only has the time between two pulses: $\tau_p = 1/f$ with f the operating frequency, Fig. 4 (c). In particular, (eq. 5) is not valid anymore. Instead, the ratio of initial to peak pulse population inversion, N_i/N_p, is now proportional the amount of excess threshold energy, x, through a term that depends on operating frequency, $f^* = \tau/\tau_p$:

$$\frac{N_i}{N_p} = x\left[\frac{1-\exp(-1/f^*)}{1-(1-\eta_E)\exp(-1/f^*)}\right] \tag{9}$$

the term in bracket in (eq. 9) is nearly constant for a given frequency f^* in the range of interest here ($N_i/N_p \geq 1.5$). For convenience, this term will be labeled $a(f^*)$ below. It increases for decreasing frequencies.

Finally the buildup time for these lasers is given by (eq. 10):

$$\tau_d = \frac{\tau_c}{a(f^*)x-1}\ln\left(\frac{\phi_p}{10}\right) \tag{10}$$

The overall behavior of the buildup time for three frequencies and various energy levels is plotted in Fig. 5 for an hypothetical laser. Buildup time increases with decreasing initial population inversion, N_i/N_p. For a given level of N_i/N_p, increasing the laser repetition rate results in an increase of the buildup time.

The laser pulse length has the same form than for the pulsed pump Q-switch, (eq. 7). It is remarkable that with this model, the pulse length is independent of frequency at first order. It only depends on the energy level, N_i/N_p, at which the laser can be pumped.

Acousto-optic Q-switches response is limited by the amount of time it takes for sound waves to propagate through the crystal. Thus, Q-switching time is rather long ($\sim$ 100 ns).

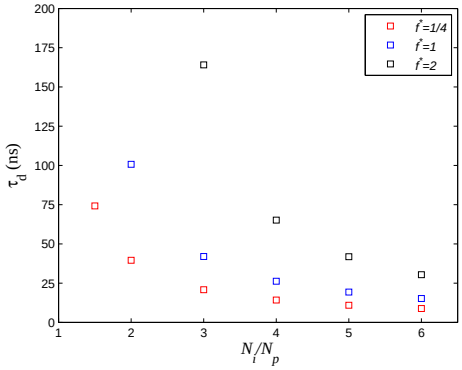

Figure 5: Behavior of buildup time for CW pump, τ_d, for $f^* = 1/4, 1, 2$ after [9].

2.3 Single Cavity Double Pulse Capabilities

Long upper-state lifetimes can be taken advantage of to generate two pulses on a single flashlamp pulse, and therefore on a single cavity with a dual Q-switch [11]. However, the maximum pulse separation is limited by the fluorescence lifetime of the crystal. Several laser manufacturers have taken advantage of this and offer double pulse capability for a single cavity. At the present time, the details of these systems dynamic are not known to the authors. However, one Nd:YLF laser was tested with this special arrangement.

3. Apparatus and Procedure

Several lasers were tested by both The George Washington University (GW) team and Doug Neal (DN) of LaVision. For testing performed by GW, the lasers were synchronized with a pulse generator from Berkeley Nucleonics (575-8C). It has a resolution of 250 ps, 200 ps RMS jitter, and a 3 ns TTL rise time. For the Nd:YLF laser, the pulses mean energy were monitored with laser power meter (Ophir NOVA II meter with F150A power sensor). The pulse temporal profile was recorded with high-speed photodiodes connected to a digital oscilloscope (Agilent MSOX-3054A). The oscilloscope has a sampling rate of up 4 GSa/s, bandwidth of 500 MHz, rise time ($10\% - 90\%$) of $\leq$ 700 ps, and internal memory of 4×10^6 points. Here the sampling rate was varied between 10 MSa/s and 4 GSa/s.

DN conducted additional tests using a LaVision programmable timing unit version 9 (PTU 9) to trigger the Q-switch (for the Nd:YLF and Nd:YAG tests) and also to trigger the firing of the flashlamp for the Nd:YAG tests. The PTU is a software-controlled synchronization unit designed and built by LaVision GmbH. The recorded jitter to periodic triggers was measured at 175 ps (RMS value). For tests using the PTU 9, the waveforms were measured using a Teledyne LeCroy WaveRunner 64Xi-A, which is a 600 MHz, 10 Gs/s oscilloscope that is capable of digitizing up to 4 channels and writing the waveforms to disk for further analysis. The WaveRunner 64Xi-A has a rise time ($10\% - 90\%$) of 500 ps.

To characterize Nd:YLF laser pulses, an amplified photodiode was used (Thorlabs DET10A). It has a rise time of 1 ns, which is ample for measuring 150 ns pulses. For Nd:YAG, a photodiode with rise time of 175 ps was used (Thorlabs SV2-FC). For these last measurements, the rise time is limited by the oscilloscopes.

The oscilloscope first channel was connected to the pulse delay generator and the TTL pulse rising edge was set to control both the laser timing and the triggering of the oscilloscope. The time reference point was set as the median of the TTL trigger rising edge. Time history of laser optical pulse was recorded on the oscilloscope second channel. Uncertainties on the time histories are dominated by the oscilloscope sampling rate. They range from 0.01 μs and 0.1 ns.

The laser pulse width is measured from the median of the rising and falling edges of the photodiode signal. Timing of laser pulse is measure differently than defined in section . It is not referred at the peak power of the pulse, but as the time at which 50% of the laser energy has been delivered. This definition leads to sightly different behavior than in section , but is more consistent with intensity of light scattered by particles. The laser pulse delay is related to the pulse buildup time, τ_d and Fig. 2, is defined as the time interval between the rising edge of the trigger pulse to the Q-switch (the $t = 0$ reference point) and the laser pulse. Pulse delay anomalies, $\delta(\Delta t)$, are the time difference between two laser pulse delays. In other words, it compares the pulse delays with respect to the command to activate the Q-switch, Fig. 12; ideally for transit-time velocimetry this should be a small fraction of the pulse length. For lasers with dual pulses per cavity capabilities, the dual pulse delay between two laser pulses is between two pulse energy mid-points. The dual pulse delay anomaly is defined as the timing difference when both pulses once the time separation, Δt, between the first and second

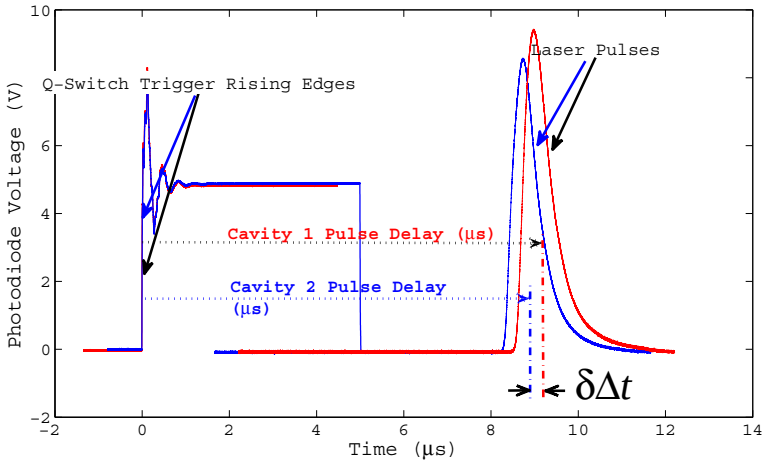

Figure 6: Pulse sequences.

pulses has been subtracted from the signals.

4. Pulsed pump Nd:YAG timing results

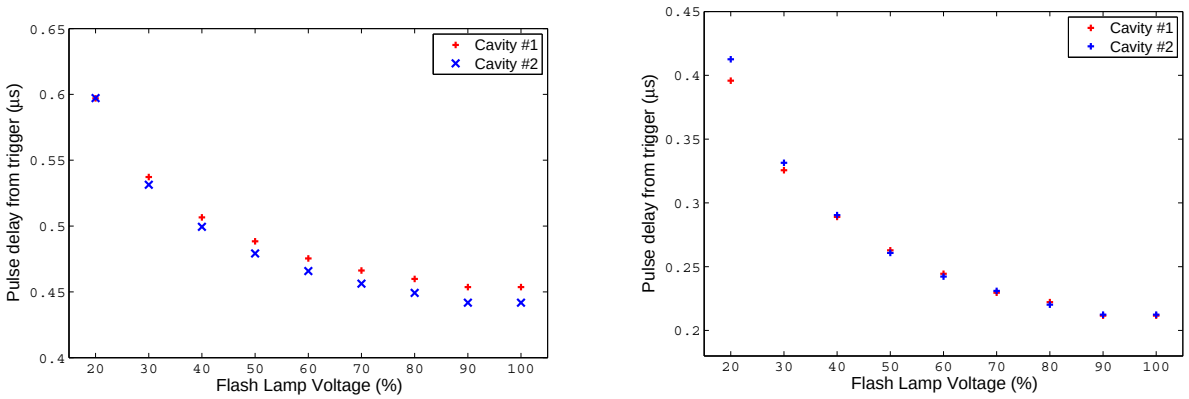

(a) Manufacturer A

(b) Manufacturer B

Figure 7: Double cavity YAG behavior from two manufacturers.

Low repetition rate Nd:YAG lasers (100 Hz or less) have been the workhorse of PIV and PTV systems in many laboratories. They have very short pulses on the order of 10 ns or less. New models are now very compact and even portable, while larger systems, employed for tomographic PIV or large field of view, can have energy in excess of 1 J per pulse! Depending on Nd:YAG manufacturer and model, laser output power is controlled by adjusting either flashlamp power, timing of Q-switch with respect to pump, or optical attenuator. Optical attenuators come in several forms and can be internal or external to the cavity. To obtain the best beam profile, it is usually recommended to optimize the Q-switch timing and attenuator and only vary the flashlamp power. Accordingly in data presented below, the laser power is controlled through the pumping rate alone.

A total of seven different double cavity Nd:YAG systems were tested; detailed results for only three of them are presented for sake of conciseness. With decreasing pumping rate, the buildup time increases, Fig. 7, in accordance with (eq. 8). It should be noted that in this figure, buildup times are reported as a function of flashlamp voltage. This is also observed for the third manufacturer, Fig. 8. This last system is over 10 years old and one cavity is only able to operate at half the power of the other. For manufacturer A, the timing anomaly was on the order of 50 ns, Fig. 7 (a), with the second cavity consistently lagging behind the first. Manufacturer B's system has timing anomalies on the order of the pulse length and depending on voltage, cavity 1 either lags or leads cavity 2. At full power, buildup time for manufacturer B is 215 ns or nearly half that of manufacturer A. Manufacturer C's system has en even shorter buildup time of less than 100 ns, Fig. 8. In this figure, the flashlamp voltage was kept the same for measurements of the same color and the laser appears to have little to no timing anomalies when adjusted for flashlamp voltage. Pulse length increases with decreasing power, Fig. 8, as inferred from the simplified model presented above. Similar behaviors are observed in other systems and it should be noted that one system has timing anomalies below 1 ns, well below a typical pulse length.

Overall, timing anomalies in low repetition rate double cavity Nd:YAG lasers are very small (50 ns maximum) and will lead to very

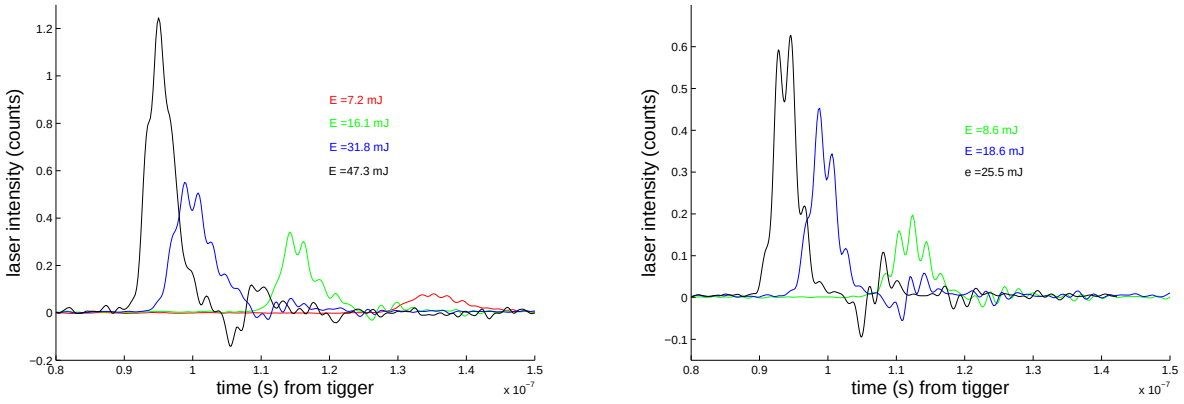

(a) Manufacturer C

(b) Manufacturer C

Figure 8: Cavities behavior. The high frequency oscillation on the pulses are due to beating longitudinal modes.

little errors except in very high speed flows were pulse separation of 5 μs or less is desired. This is also very dependent on the laser manufacturer. Dual pulse single cavities Nd:YAG laser were not tested at this time.

Finally, optical attenuator may offer a convenient mean of controlling the laser power at the expense (to some extent) of the beam quality. Internal optical attenuator will increase losses in the laser cavity, resulting in different critical inversion population, N_c. This may, in turn, affect the buildup time of Q-switches. On the other hand, external optical attenuators have the potential of not affecting buildup time, which for some PIV applications is more important than beam quality. Unfortunately, at this time neither of these systems have been tested by the authors.

5. Continuous pump Nd:YLF timing results

Nd:YLF lasers have become the standard to perform PIV in the 1-20 kHz frequency range. They have longer pulses than low repetition rate Nd:YAG lasers, varying between 100-200 ns at full power. They are now relatively affordable and are best paired with widely used high-speed CMOS cameras. Nd:YLF lasers are available from several manufacturers either as single-cavity units with dual pulse capability, or as dual cavity laser. Three lasers from 2 manufacturers were extensively tested. Two were from manufacturer A and one from manufacturer B. This last laser has both characteristics combined, i.e. it is a double cavity system and each cavity has a double pulse option. It can be used as a regular dual cavity laser or can generate up to 4 lasers pulses per cycles with independently controllable time delays. The pulse delays are set at 4 μs on each cavity for manufacturer A lasers and at 2.6 μs for manufacturer B system. In dual pulse per cavity mode, only one trigger pulse is sent to the control unit. The first pulse delay is set electronically as 7.6 μs and the pulse separation, Δt, is entered electronically.

For dual cavity systems, the lasers behave consistently for manufacturer A, but very differently than for manufacturer B, see Fig. 9. Their buildup time is also significantly longer than Nd:YAG lasers. The absolute pulse delay for each cavity is shown in Fig. 9 (a-c) for the three lasers under test here. Fig. 9 (d) presents pulse delay anomaly between the two cavities for the third laser.

Lasers from manufacturer A have increasing buildup time as the operating frequency increases, Fig. 9 (a-b). The trend is similar for both systems as would be expected. As the diode current decreases the buildup time increases in agreement with the continuous pump Q-switch simple model, (eq. 10). The timing anomaly between the two cavities ranges from 0.0 to 0.3 μs at full power as the frequency is varied. When pumping rate is reduced, the timing anomaly increases and can exceed 1 μs , for the first laser at 10 kHz and 10% of available power. The length of the pulses increases slightly with operating frequency, it also increases significantly with decreasing pump power. Finally, it should be noted that a recent model from this manufacturer (the data of which are not reported here) appears to have a built in photodiode and very small timing uncertainties when the laser is operated at maximum pumping rate.

The laser from the second manufacturer has consistent behavior with diode current, i.e. pulse length (not displayed here) and buildup time is solely controlled by the diode pump rate, 9 (c), for a repetition rate superior to 500 Hz. Time delays are constant and independent of the laser operating frequency. They vary between 2.5 and 3.7 μs depending only the optical pump power. However, the time delays vary independently for each cavity probably due to difference between cavity losses and acousto-optical Q-Switches. The variation in buildup times ranges between 50 and 300 ns for a repetition rate superior to 500 Hz. As a result, for this system the pulse delay anomalies are non-monotonic, but with further measurements a polynomial fit can be interpolated to calibrate this instrument and correct for these timing anomalies either prior to taking the measurements or in a post-processing phase.

In dual pulse mode, the laser cavity must be extensively calibrated to guarantee appropriate timing separation, and energy distribution between the pulses. The dual pulse controller of manufacturer B allows controlling the energy ratio (such as 30% first pulse 70% second pulse), but this ratio is accurate for only for a given Δt, pump energy, and frequency, preselected at the factory. If the laser needs to be employed with different parameters, which is often the case, the parameters of the controller must be re-calibrated. Here calibration is an iterative process. The laser diodes are set at full power and the desired Δt and frequency are inputted. The energy of each pulse is measured by integrating the pulse profile recorded with a high-speed photodiode while the energy ratio between the pulses, set by the

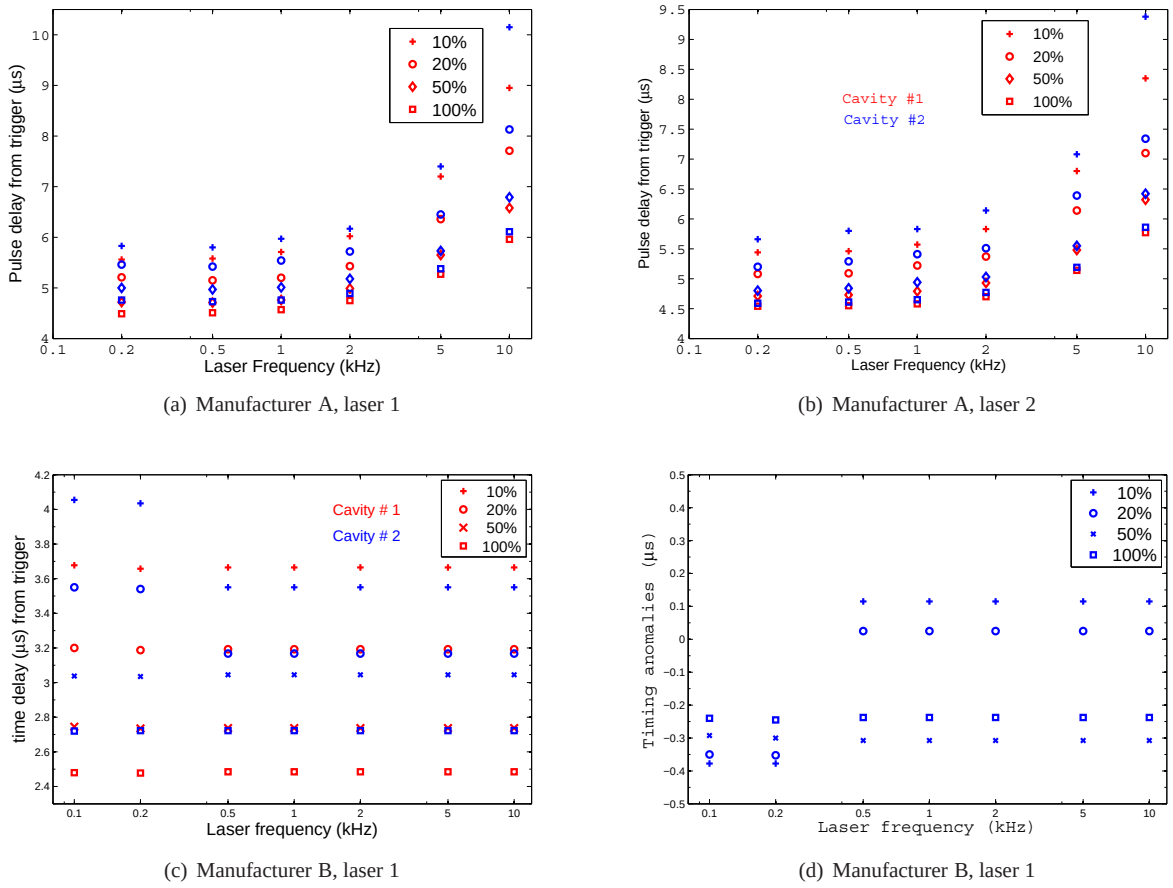

(a) Manufacturer A, laser 1

(b) Manufacturer A, laser 2

(c) Manufacturer B, laser 1

(d) Manufacturer B, laser 1

Figure 9: Nd:YLF behavior from 2 different manufacturers.

controller is varied. Typically 5 data points are needed to perform a polynomial fit of the power ratio measured vs. the values entered in the controller. The user is then able input the proper pulse power ratio in order to have two equal energy laser pulses. Once this is done, the pulse separation must be checked again, and the procedure repeated if the timing has changed.

Here calibration was conducted for $\Delta t = 20\ \mu s$. For Δt between 5 and 30 μs , the repartition of the energy between the two pulses is fairly consistent as well as the timing anomaly which varies between 0.6 and 0.7 μs , Fig. 10. This represents between 2 and 10% of Δt! As the time separation between the pulses increases, the spread of the energy and pulse separation varies significantly. For $\Delta t \geq 30\ \mu s$ a new series of calibrations is needed. The laser has been observed to behave consistently, though, and can be calibrated once for a set of Δt at a given operating frequency.

To decrease the energy of the pulses, beam can be attenuated with beam splitters, hence it is not necessary to recalibrate the laser for reduced power. Furthermore, the laser needs a certain level of pump energy to be able to produce two pulses per pumping cycle.

Jitter has been measured on manufacturer B laser, Fig 11. At maximum power, the overall pulse is $\sim$ 125 ns long, Fig 11 (a). For 8 individual pulses, the maximum separation between the raising edges is 1.5 ns, Fig 11 (b). This jitter corresponds to an RMS value of 1.15 ns at 95% confidence, which is within the specifications of the manufacturer (3 ns). Furthermore, it should be noted that this jitter is a small fraction of the overall pulse length and that for these lasers jitter is negligible.

For continuous pump q-switch lasers, it is also possible to decrease the beam energy by increasing the off-time of the Q-switch (Fig. 4), thus preventing the number of atoms in the upper-state to build up. Since, this affects the population inversion, the buildup time response will also be changing with power. Finally, it should be noted that continuously pumped high-speed Nd:YAG lasers with repetition rates in excess of 10 kHz were not tested.

6. Conclusion and Recommendations

Timing errors associated with low-speed Nd:YAG and Nd:YLF lasers have been characterized and quantified. They are inherent to the nature of Q-switches employed in these pulsed lasers. They are dominated by bias errors, with jitter being negligible. The Nd:YAG lasers, which are typically used in PIV experiments that require acquisition rates up to about 100 Hz, show a bias error that is a function of the cavity energy only. Measured discrepancies are up to 50 ns. The Nd:YLF lasers, which primarily come in two different configurations show a bias error that is significantly larger and can exceed 1 μs . These lasers are typically used in time-resolved PIV (TR-PIV) experiments that require acquisition rates from 100 Hz - 10,000 Hz (and increasingly greater). Single-cavity dual pulse

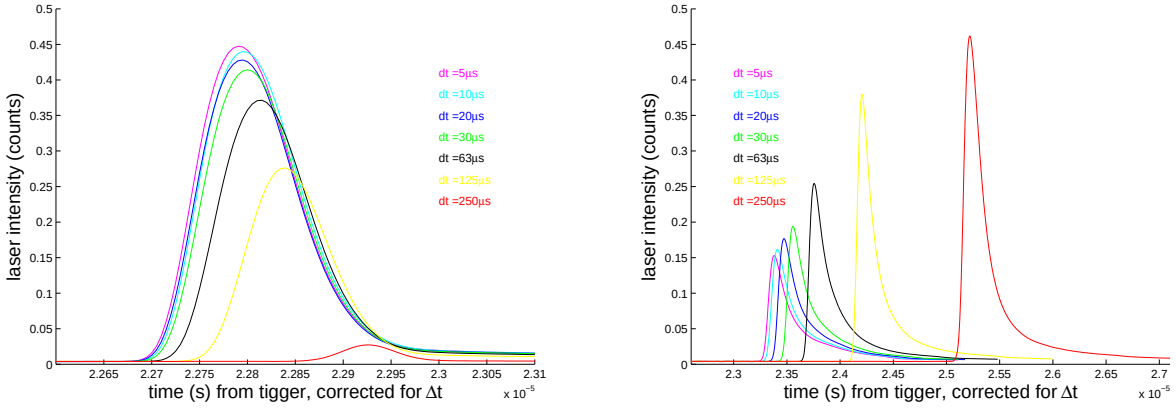

(a) 1^{st} Pulse (b) 2^{nd} Pulse

Figure 10: Nd:YLF of manufacturer B in dual pulse per cavity mode.

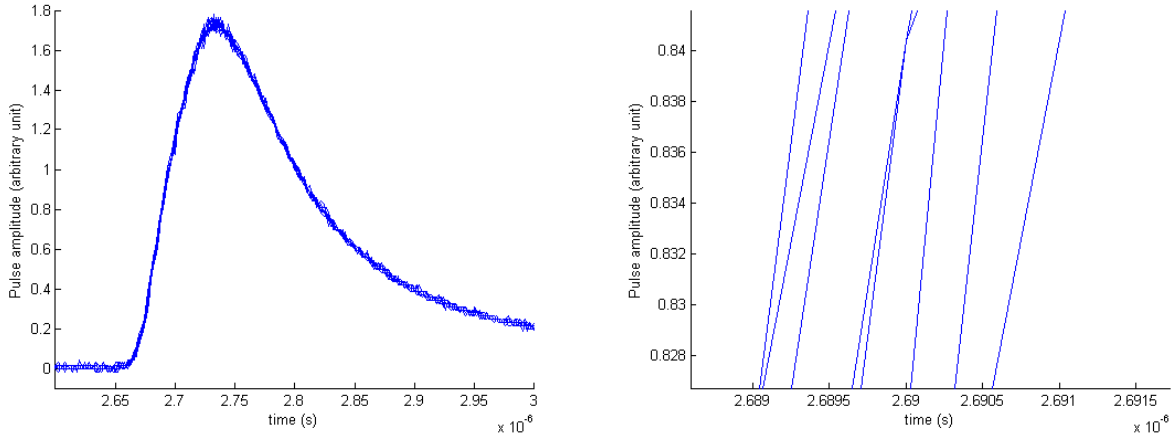

(a) Manufacturer B (b) Manufacturer B, zoomed section

Figure 11: Jitter of Nd:YLF for the second manufacturer.

Nd:YLF lasers have timing errors that are a function of the diode current, frequency, and pulse separation. If the system is not carefully calibrated, these errors range from 0.4 μs up to several μs . These lasers have become popular in recent years since they provide a cost-effective solution for collecting TR-PIV data; however, their timing bias could pose problems for many PIV experiments if special precautions are not taken. Dual-cavity Nd:YLF lasers have timing errors that are a function of the diode current and frequency. These errors are between 0 and 1.5 μs for the data collected here. No data were collected on high-speed Nd:YAG lasers that operate at frequencies greater than 10 kHz.

Since the errors introduced by all of these layers are systematic in nature, they can be corrected for in a straightforward manner. For low-speed Nd:YAG lasers, a good practice is to always run the laser with the maximum flash lamp voltage and the minimum flash lamp-to-Q-switch delay. This mode of operation will also result in the best beam profile, which in turn creates a uniform light sheet. The excess energy that is not needed for the experiment can be discarded by employing a polarizing attenuator directly downstream of the beam combining optics. Several manufacturers offer this as an add-on option and these attenuators allow for the energy to be adjusted continually between full power (100%) and a very lower power ($\approxeq$ 0%). Additionally, the authors are aware of at least one manufacturer who offers an after-market attenuator that can easily be retrofit onto virtually any existing laser without having to undertake risky alterations to the existing optics.

Nd:YLF lasers pose a greater challenge for a reasonable and cost-effective solution, which is especially problematic given that the magnitude of the error is much greater. These errors exist in both variations (dual cavity and single cavity) and they are most pronounced when operated at lower diode currents. This represents a problem for the experimentalist who needs to reduce the laser power to prevent damaging an experiment (which can easily result in starting a fire) or reduce the light intensity to avoid damaging the camera sensor. A good practice is therefore to carefully calibrate Nd:YLF timings and following manufacturer's recommendations, operate these lasers at full diode current. Similar to an Nd:YAG laser, this mode of operation will also result in the best beam profile, creating a uniform light sheet. To the authors knowledge no laser manufacturer provides an attenuator for their Nd:YLF laser.

One alternative solution for Nd:YLF lasers exists by dividing off the excess laser energy through a beam-splitter (i.e. 80-20, 70-30, etc). However, this is not an ideal solution as it cannot be easily adjusted and to equip a lab with a whole range of different beam

splitters is cost-prohibitive for many researchers. The authors are aware that laser manufacturers are currently working at minimizing these systematic errors. The best practice for researchers using an Nd:YLF laser is obtain a fast photodiode and high quality digital oscilloscope (at least 100 MHz) so they can correct for the bias errors for a given experiment. This analysis can be made either *a priori* or *a posteriori*, so older datasets can be corrected. Additionally the experimentalist is not penalized for changing the laser settings midway through a measurement campaign. The downside to this approach is that equipment is expensive and the characterization requires time (additional time not focused on the primary research tasks). It is expected that the magnitude of the error will remain relatively constant over time; however, as a laser ages the output power will normally decrease for a given diode current. A common strategy is to increase the diode current to account for this reduced power or to correct for an imbalance in the pulse energy of each cavity. It is reasonable to expect that this could also affect the timing bias errors, but the authors have not examined these long-term effects in detail.

Another possible solution for both Nd:YAG and Nd:YLF lasers could be to measure and correct for timing anomalies electronically, via a circuit which introduces additional time delays when needed. It should be noted that at least one laser manufacturer has recently begun installing a photodiode inside the laser head. This photodiode can be accessed through a small BNC connector located at the back of the laser head.

Figure 12: Externally mounted connector for internal photodiode on certain Nd:YLF laser models

Acknowledgments

The authors would like to thank Radomir Beslac and Uwe Dierksheide of LaVision GmbH for their assistance with measuring and documenting the timing data for a wide range of commercially available lasers. Additional thanks to Zohaib Hasnain, Andrew Lind and colleagues from the University of Maryland for allowing usage of their lab and lasers for some of the measurements. This research was partially supported using funding received from the DOE Office of Nuclear Energy's Nuclear Energy University Programs.

REFERENCES

[1] B. H. Timmins, B. W. Wilson, B. L. Smith, and P. P. Vlachos. A method for automatic estimation of instantaneous local uncertainty in particle image velocimetry measurements. *Experiments in Fluids*, 53 113347, 2012.

[2] B. M. Wilson and B. L. Smith. Taylor-series and monte-carlo-method uncertainty estimation of the width of a probability distribution based on varying bias and random error. *Measurement Science and Technology*, 24:035301, 2013.

[3] B. M. Wilson and B. L. Smith. Uncertainty on PIV mean and fluctuating velocity due to bias and random errors. *Measurement Science and Technology*, 24:035302, 2013.

[4] A. Sciacchitano, B. Wieneke, and F. Scarano. PIV uncertainty quantification by image matching. *Measurement Science and Technology*, 24:045302, 2013.

[5] J. J. Charonko and P. P. Vlachos. Estimation of uncertainty bounds for individual particle image velocimetry measurements from cross-correlation peak ratio. *Measurement Science and Technology*, 24:065301, 2013.

[6] R. J. Adrian and J. Westerweel. *Particle Image Velocimetry*. Cambridge Aerospace Series, 2010.

[7] J. M. Foucaut and M. Stanislas. Some considerations on the accuracy and frequency response of some derivative filters applied to particle image velocimetry vector fields. *Measurement Science and Technology*, (13):1058–1071, 2002.

[8] M. C. Leftwich, E. D. Tytell, A. H. Cohen, and A. J. Smits. Wake structures behind a swimming robotic lamprey with a passively flexible tail. *The Journal of Experimental Biology*, (215):416–425, 2012.

[9] O. Svelto. *Principles of Lasers*. Chapter 8. $4^{th}ed.$, Springer, 1998.

[10] R. Paschotta. *Encyclopedia of Laser Physics and Technology*. Wiley-VCH, 2008.

[11] R. Spooren. Double-pulse characteristics of a single-oscillator Nd:YAG laser affecting its performance in TV holography. *Applied Optics*, (31)2:208–216, 1992.